

Mechanistic understanding of the effect of rigidity percolation on structural relaxation in supercooled germanium selenide liquids

E. L. Gjersing and S. Sen

Department of Chemical Engineering & Materials Science, University of California at Davis, Davis, California 95616, USA

R. E. Youngman

Glass Research Division, Corning Inc., Corning, New York 14831, USA

(Received 30 April 2010; revised manuscript received 5 July 2010; published 26 July 2010)

High-resolution ^{77}Se nuclear magnetic resonance spectroscopy is used to investigate the rotational dynamics of Se atoms in $\text{Ge}_x\text{Se}_{100-x}$ supercooled liquids with $5 \leq x \leq 23$. The Se atoms in Se-Se-Se linkages are found to be significantly more mobile compared to those in Ge-Se-Se/Ge linkages. The time scale of the rotational dynamics of Se-Se-Se linkages and its temperature dependence are nearly identical for liquids with $x \leq 17$ but the time scale displays an abrupt increase for the liquids with $x=20$ and 23, at and above the rigidity percolation threshold. Such a dynamical transition is shown to be consistent with a sudden elastic stiffening of the atomic network of $\text{Ge}_x\text{Se}_{100-x}$ supercooled liquids at the percolation threshold.

DOI: [10.1103/PhysRevB.82.014203](https://doi.org/10.1103/PhysRevB.82.014203)

PACS number(s): 61.43.Fs, 81.05.Kf, 82.56.-b

I. INTRODUCTION

The application of the concept of rigidity percolation has received a great deal of research attention in recent years in explaining the composition dependence of a wide range of physical properties in network glasses on the basis of topology and connectivity of the network.^{1–16} Initially the rigidity percolation model was put forward to explain the transition of an elastic network from floppy to rigid state when the number of degrees of freedom per atom becomes equal to the number of interatomic force-field constraints.^{1–3} The network is floppy when the number of degrees of freedom is higher than the number of constraints and it is rigid when the reverse holds true. The rigidity of the network is therefore controlled by its connectivity and it can be shown that the floppy to rigid transition takes place when the average coordination number $\langle r \rangle = 2.4$ at which point the fraction of floppy modes goes to zero.^{1–3} Phillips was the first to suggest that the glass-forming tendency of covalently bonded chalcogenide networks would be maximized when $\langle r \rangle = 2.4$.¹ This model has since been used extensively to elucidate the compositional variation in mechanical, thermodynamic, transport, and electronic properties in covalent amorphous chalcogenide networks simply on the basis of $\langle r \rangle$, irrespective of the chemical composition. More recently the application of such models has been extended to oxide glass networks as well.^{13,14}

It is to be noted that in the original rigidity percolation model no thermal energy is available to the network to overcome the interatomic force-field constraints, i.e., the model is strictly valid only at $T=0$ K. Therefore, ideally the model cannot be used to predict temperature-dependent dynamical properties such as fragility, glass-forming ability, and glass transition temperature T_g . However, strong correlations between $\langle r \rangle$ and such dynamical properties have been experimentally observed in covalent chalcogenide networks in binary and ternary glass-forming liquids in Ge-As-Se system that have been linked to the concept of mean-field rigidity percolation.^{7,10–18} Naumis has recently conjectured that

floppy modes in networks with $\langle r \rangle < 2.4$ may provide channels in the potential-energy landscape for structural rearrangements in the liquid that in turn would govern its configurational entropy and fragility.^{11,12} Recently, Mauro and co-workers^{13–15} have proposed a modified version of the Naumis model based on temperature dependence of interatomic force-field constraints to explain the composition dependence of fragility and T_g in a variety of oxide and non-oxide network liquids including those in the binary Ge-Se system. However, none of these models provides a direct mechanistic understanding of the dynamical processes at the atomic scale that are responsible for viscous flow and shear relaxation and glass transition in networks with widely different $\langle r \rangle$ values. It also remains an open question whether such dynamical processes, once identified, would show a transitional behavior that is coincident with the rigidity percolation threshold at $\langle r \rangle = 2.4$. Here we report the results of a high-temperature ^{77}Se nuclear magnetic resonance (NMR) spectroscopic study of $\text{Ge}_x\text{Se}_{100-x}$ glasses and supercooled liquids with $5 \leq x \leq 23$ that has been carried out to investigate the temperature-dependent dynamics of Se atoms near the glass transition range as a function of $\langle r \rangle$. Considering Ge and Se atoms to be four- and two-coordinated, respectively, the $\langle r \rangle$ values of these compositions range between 2.10 and 2.46.

II. EXPERIMENTAL

$\text{Ge}_x\text{Se}_{100-x}$ glasses with $x=5, 10, 17, 20$, and 23 ($\langle r \rangle = 2.10, 2.20, 2.34, 2.40$, and 2.46, respectively) were synthesized by melting mixtures of the constituent elements Ge and Se with $\geq 99.995\%$ purity (metals basis) in evacuated (10^{-6} Torr) and flame sealed fused silica ampoules at temperatures ranging between 1000 and 1200 K for at least 24 h in a rocking furnace. The ampoules were quenched in water and subsequently annealed for 1 h at the respective T_g 's. T_g was determined to within ± 2 K by differential scanning calorimetry using a heating rate of 10 K/min and were found to be 330 K, 361 K, 411 K, 430 K, and 450 K for glasses

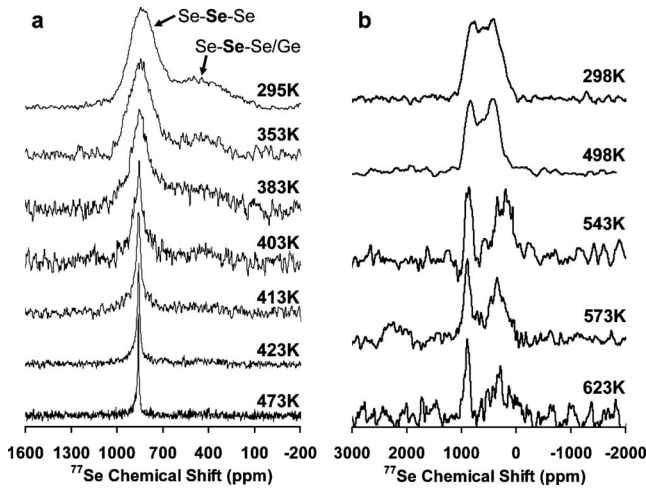


FIG. 1. ^{77}Se NMR spectra of (a) $\text{Ge}_{10}\text{Se}_{90}$ and (b) $\text{Ge}_{20}\text{Se}_{80}$ glasses and supercooled liquids, as a function of temperature. The corresponding temperatures are indicated alongside each spectrum.

with $x=5, 10, 17, 20$, and 23 , respectively. Variable temperature ^{77}Se NMR experiments were carried out on $x=5, 17, 20$, and 23 glasses and supercooled liquids using a Bruker Avance-500 solid-state NMR spectrometer operating at a Larmor frequency of 95.4 MHz (11.7 T) and a high-temperature NMR probe (Doty Inc.). Crushed glass samples were packed in a boron nitride capsule that was inserted into a 7 mm Si_3N_4 rotor. N_2 gas boil off from a high-pressure liquid-nitrogen Dewar was used for temperature control of the sample. For the $\text{Ge}_{10}\text{Se}_{90}$ sample variable temperature ^{77}Se NMR experiments were carried out on a Chemagnetics NMR spectrometer with a Chemagnetics magic angle spinning (MAS) probe (4 mm ZrO_2 rotors) operating at a Larmor frequency of 95.4 MHz (11.7 T). The temperature of both probes was calibrated externally using the well-known temperature dependence of the ^{207}Pb chemical shift of $\text{Pb}(\text{NO}_3)_2$, before and after the ^{77}Se NMR measurements.¹⁹ For $T \leq 1.3T_g$ a Hahn-echo pulse sequence ($\pi/2-\tau-\pi$ acquisition) was employed for spectral acquisition with $\pi/2$ pulse length of $2.6\text{ }\mu\text{s}$ and $\tau=63\text{ }\mu\text{s}$ and recycle delays of 60 s . For spectra collected at $T \geq 1.3T_g$ single pulse experiments were employed along with shorter delay times of 1 s for rapid data collection in order to avoid crystallization. Approximately $1000\text{--}1500$ free induction decays (FID) were averaged to obtain each ^{77}Se spectrum at temperatures below T_g while $150\text{--}500$ FIDs were averaged to obtain spectra at $T > T_g$. All ^{77}Se NMR chemical shifts are reported with respect to an external reference of saturated H_2SeO_3 liquid.

III. RESULTS AND DISCUSSION

The ^{77}Se NMR spectra of $\text{Ge}_{10}\text{Se}_{90}$ glass and supercooled liquid are shown as an example in Fig. 1(a). The spectrum acquired at room temperature displays two distinct resonances centered around ~ 830 and 450 ppm . Previous ^{77}Se NMR spectroscopic studies based on a wide range of $\text{Ge}_x\text{Se}_{100-x}$ glasses and crystalline model compounds have unequivocally assigned the 830 and 450 ppm resonances to

Se environments with two Se nearest neighbors, i.e., Se-Se-Se sites and to Se environments with one or two Ge nearest neighbors, i.e., Ge-Se-Se/Ge sites, respectively.^{20–22} The full widths at half maximum (FWHM) of these two resonances are found to be ~ 200 and 500 ppm , respectively. Simulation of this spectrum with two Gaussian peaks centered at 830 and 450 ppm indicates that $\sim 38\%$ and 62% of the Se atoms in this glass belong to the Ge-Se-Se/Ge and Se-Se-Se sites, respectively, consistent with previous reports. This ^{77}Se NMR line shape does not change appreciably upon heating to up to 353 K [Fig. 1(a)]. However, with further increase in temperature to 383 K ($T_g=361\text{ K}$) the FWHM of the resonance corresponding to the Se-Se-Se sites decreases rapidly and monotonically until at the highest temperature of measurement (473 K) it is only $\sim 30\text{ ppm}$ indicating motional narrowing [Fig. 1(a)]. Motional narrowing of ^{77}Se NMR signal in binary Ge-Se supercooled liquids at temperatures above T_g was also observed in a previous study by Eckert and co-workers.²³

It is important to note that the use of short recycle delay times for ^{77}Se NMR data collection at $T \geq 1.3T_g$ results in suppression of the signal from Ge-Se-Se/Ge sites that are characterized by significantly longer spin-lattice relaxation times than those of the Se-Se-Se sites, consistent with the high mobility of the latter (vide infra). However, the integrated area under the Se-Se-Se resonance does not change appreciably over this temperature range. This result indicates the lack of any chemical exchange of Se atoms between the Se-Se-Se and Ge-Se-Se/Ge sites due to bond breaking events. Therefore, the motional narrowing of the Se-Se-Se resonance with increasing temperature clearly implies rapid rotation of the selenium chain segments in the structure of the supercooled $\text{Ge}_{10}\text{Se}_{90}$ liquid. On the other hand, the Ge-Se-Se/Ge type selenium environments appear to remain relatively rigid in this temperature range. Similar dynamical behavior has recently been reported by Lucas *et al.*²⁴ in a liquid of identical composition. In the present study this contrasting temperature-dependent behavior of the ^{77}Se NMR line shapes for the two types of Se sites is found to be universal for all $\text{Ge}_x\text{Se}_{100-x}$ compositions, regardless of the chemistry, and to be completely reversible upon cooling back down to ambient temperature. This situation is evident in the ^{77}Se NMR spectra of $\text{Ge}_{20}\text{Se}_{80}$ glass and supercooled liquid collected over a temperature range between ambient and 623 K as shown in Fig. 1(b). It should also be noted that with increasing temperature the peak position of the Se-Se-Se resonance in the ^{77}Se MAS NMR spectra shifts to lower field or higher chemical shifts at a rate of $\sim 0.18\text{ ppm/K}$. Our ^{77}Se NMR studies on pure Se liquid indicate that such temperature-dependent chemical shift results from thermal-expansion effects.

The temperature dependence of the FWHM of the static spectra for the Se-Se-Se resonance is compared in Fig. 2 for all $\text{Ge}_x\text{Se}_{100-x}$ compositions. It is immediately apparent from this comparison that the three compositions with $x=5, 10$, and 17 ($\langle r \rangle=2.10, 2.20$, and 2.34 , respectively) display nearly identical temperature dependence of motional narrowing of the linewidth when the temperature is scaled with respect to T_g (Fig. 2). The narrowing of the linewidth begins at $\sim T_g$ ($T/T_g=1$) and continues at a rate of $\sim 2.5\text{ ppm/K}$ to

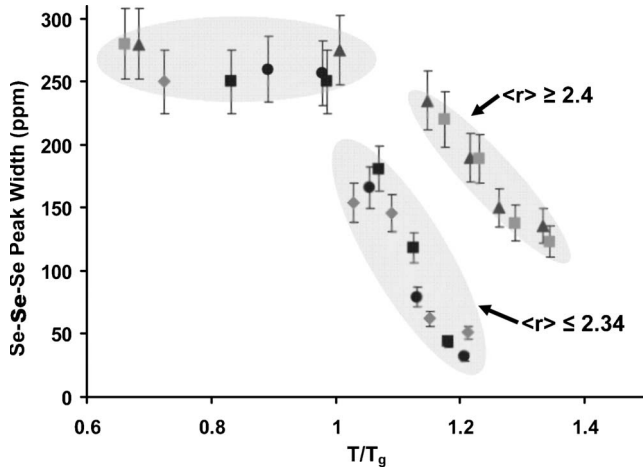


FIG. 2. Full width at half maximum of the ^{77}Se NMR resonance corresponding to the Se-Se-Se site as a function of temperature normalized to T_g for $\text{Ge}_5\text{Se}_{95}$ (black circles), $\text{Ge}_{10}\text{Se}_{90}$ (black squares), $\text{Ge}_{17}\text{Se}_{83}$ (light gray diamonds), $\text{Ge}_{20}\text{Se}_{80}$ (dark gray triangles), and $\text{Ge}_{23}\text{Se}_{77}$ (light gray square).

temperatures of at least up to $T/T_g \sim 1.2$. In stark contrast, the supercooled $\text{Ge}_{20}\text{Se}_{80}$ and $\text{Ge}_{23}\text{Se}_{77}$ liquids with $\langle r \rangle = 2.40$ and 2.46 , respectively, i.e., with average coordination numbers at and above the nominal rigidity percolation threshold, show no detectable narrowing at T_g and a significantly lower rate of motional narrowing (~ 1.3 ppm/K) of the Se-Se-Se linewidth compared to that observed for the supercooled liquids with $\langle r \rangle \leq 2.34$ (Fig. 2). The difference in the line narrowing behavior is especially evident at $T/T_g \sim 1.2$ where the Se-Se-Se linewidth for the $\text{Ge}_{20}\text{Se}_{80}$ and $\text{Ge}_{23}\text{Se}_{77}$ liquids is ~ 210 ppm while that for the other three compositions are only ~ 50 ppm. This large and abrupt change in the dynamical behavior of selenium chain fragments upon a small change in Ge content from 17 to 20 at. % coincides with the percolation threshold that is predicted by the rigidity percolation model to be located at $x = 20$ as discussed above.

Further insight into the nature of the selenium chain dynamics associated with the observed motional line narrowing in the ^{77}Se NMR spectra can be gained by quantitative dynamical modeling of the Se-Se-Se resonance line shapes of the supercooled $\text{Ge}_x\text{Se}_{100-x}$ liquids. Previous structural studies have conclusively shown that the linewidths of the ^{77}Se NMR spectra of $\text{Ge}_x\text{Se}_{100-x}$ glasses are primarily controlled by the chemical shift distribution resulting from structural disorder in glasses.^{20,21} The time scales of rotational motion of selenium chain segments responsible for the motional narrowing of the Se-Se-Se resonance can then be estimated by simulating this line shape using a standard model of random cross exchange between a sufficiently large number of “sites” under the line shape. The room-temperature ^{77}Se NMR line shape corresponding to the Se-Se-Se resonance was simulated using 30–60 equally spaced “sites” (N) under a Gaussian envelope centered at 830 ppm. These sites represent glassy structural disorder in the form Se-Se-Se environments with a distribution of local geometries that results in a heterogeneously broadened ^{77}Se NMR line shape. The general expression for equation of motion of magnetization

$M_j(t)$ for any individual site j with resonance frequency ω_j that is exchanging with sites k can be written as²⁵

$$\frac{dM_j(t)}{dt} = i\omega_j M_j(t) - [M_j(t)/T_{2j}] + \sum_k \Pi_{jk} M_k(t). \quad (1)$$

In this expression T_{2j} is the inverse of the linewidth of site j without any exchange and Π_{jk} is the exchange matrix. For N sites exchanging at a rate of $1/\tau_{\text{NMR}}$, the exchange matrix $\Pi_{jk} = 1/\tau_{\text{NMR}}(1 - N\delta_{jk})$. Since the probability for exchange of one site with any one of the other $N-1$ sites is $1/\tau_{\text{NMR}}$ the off-diagonal elements of this exchange matrix ($\delta_{jk}=0$) are one and the diagonal elements are $-(N-1)$ such that $\sum_j \Pi_{jk} = 0$. The final expression for the line shape $g(\omega)$ resulting from cross exchange between N distinct sites is given by: $g(\omega) = \mathbf{1} \cdot \mathbf{A}(\omega)^{-1} \cdot \mathbf{W}$, where $\mathbf{1}$ is the unit matrix, $\mathbf{A}(\omega) = i(\omega\mathbf{1} - \omega) - \Pi$, ω includes the T_2 term, and \mathbf{W} is the initial probability vector, i.e., populations or relative fractions of the N sites. In the present case N was varied between 30 and 60, and $1/\tau_{\text{NMR}}$ is the exchange frequency between the N Se sites. The value of T_{2j} of 0.1 ms was obtained from simulation of the room-temperature spectrum with an exchange frequency ($1/\tau_{\text{NMR}}$) of zero and has been treated as a constant for all sites in all of the simulations at higher temperatures. The average rotational exchange time scale τ_{NMR} was found to be independent of N in the chosen range $30 \leq N \leq 60$. The motionally narrowed Se-Se-Se line shapes for all $\text{Ge}_x\text{Se}_{100-x}$ supercooled liquids at temperatures $T \geq T_g$ were simulated using a temperature-dependent average exchange rate $1/\tau_{\text{NMR}}$ between the constituent Se-Se sites. The shift in the Se-Se-Se peak position due to thermal expansion has also been incorporated into all the simulations. An example of a comparison between the experimental and simulated ^{77}Se NMR line shapes for the Se-Se-Se resonance is shown in Fig. 3 for the $\text{Ge}_{10}\text{Se}_{90}$ glass and the supercooled liquid at different temperatures.

The T_g -scaled temperature dependence of the τ_{NMR} values corresponding to the rotational motion of selenium chain segments obtained from these simulations are compared in Fig. 4 to that of the shear relaxation time scales τ_{shear} for the four supercooled liquids studied here. The τ_{shear} values are obtained from the viscosity data available in the literature²⁶ for these compositions using the Maxwell relation: $\tau_{\text{shear}} = \eta/G_\infty$. In this expression η is the shear viscosity and G_∞ is the infinite frequency shear modulus, taken to be a temperature-independent constant with values between 4.3 and 6.7 GPa.²⁷ It is clear from Fig. 4 that the τ_{NMR} time scales for all $\text{Ge}_x\text{Se}_{100-x}$ compositions with $23 \geq x \geq 5$ are significantly decoupled from τ_{shear} at relatively low temperatures within the range of $1.0 \geq T_g/T \geq 0.75$ and the degree of decoupling rapidly increases with decreasing temperature. The corresponding activation energy for τ_{NMR} is ~ 79 kJ/mol which is significantly lower than that (~ 215 – 235 kJ/mol) associated with τ_{shear} at temperatures in the glass transition range. While the magnitude and activation energy of τ_{shear} progressively change with composition, the activation energy of τ_{NMR} remains practically unchanged for all compositions in this temperature range. However, such a temporal decoupling between fast motion of

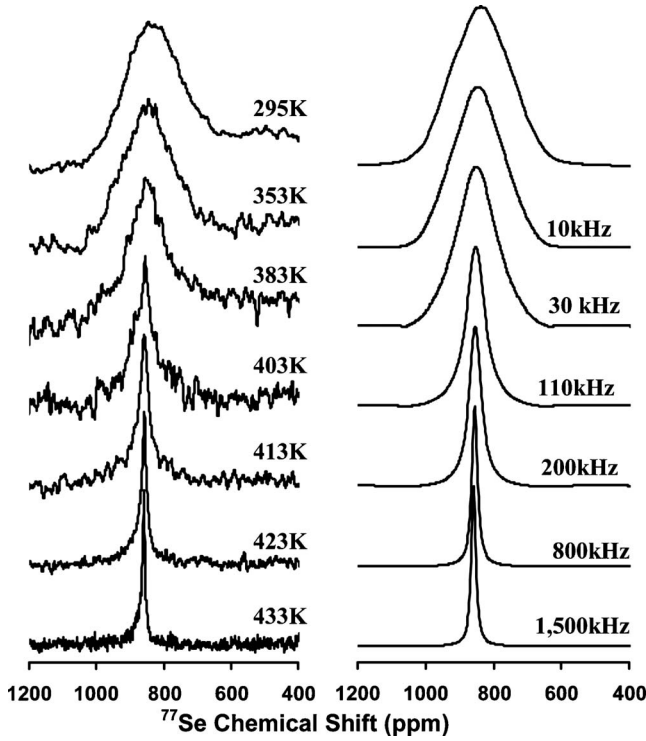


FIG. 3. Experimental (left) ^{77}Se NMR line shapes corresponding to the Se-Se-Se site in $\text{Ge}_{10}\text{Se}_{90}$ glass and supercooled liquid at the temperatures indicated and the corresponding simulated line shapes (right). The corresponding rotational exchange frequencies ($1/\tau_{\text{NMR}}$) are given alongside each simulated line shape.

selenium chain segments and shear relaxation is not unexpected in these systems where the primary or α relaxation time is presumably controlled by the relaxational processes of the Ge-Se backbone consisting of corner- and edge-shared GeSe_4 tetrahedra.

More interestingly, and consistent with the motional narrowing behavior of the Se-Se-Se resonance mentioned above, the magnitude of τ_{NMR} shows an abrupt increase by ~ 1.5 orders of magnitude for the $\text{Ge}_{20}\text{Se}_{80}$ and $\text{Ge}_{23}\text{Se}_{77}$ liquids (Fig. 4). It should be noted that τ_{NMR} displays an Arrhenius behavior in its temperature dependence that can be expressed as $\tau_{\text{NMR}} = \tau_0 [\exp(E_{\text{NMR}}/k_B T)]$, where E_{NMR} is the activation energy and τ_0 is the inverse of the attempt frequency. Since E_{NMR} does not change appreciably with composition, the abrupt increase in τ_{NMR} must represent a corresponding increase in τ_0 in the $\text{Ge}_{20}\text{Se}_{80}$ and $\text{Ge}_{23}\text{Se}_{77}$ liquids. Arrhenius fits to the τ_{NMR} data indicate that τ_0 increases from $10^{-13.5}$ s for compositions with $17 \geq x \geq 5$ to $10^{-12.0}$ s for the $\text{Ge}_{20}\text{Se}_{80}$ and $\text{Ge}_{23}\text{Se}_{77}$ supercooled liquids (Fig. 4). Therefore, the establishment of rigidity percolation in a network results in a sudden decrease in the attempt frequency for structural rearrangement processes such as rotational dy-

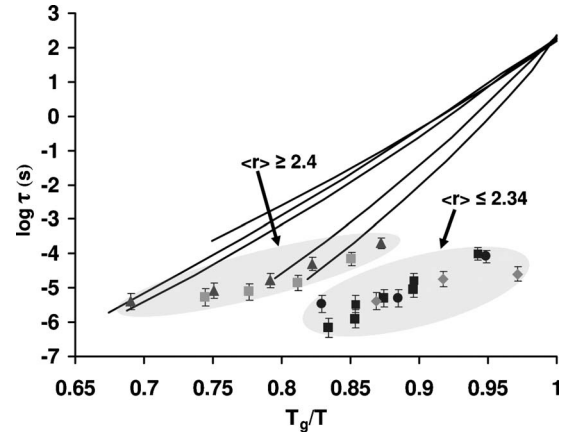


FIG. 4. Comparison between τ_{NMR} (symbols) and τ_{shear} (smooth curves) values for $\text{Ge}_5\text{Se}_{95}$ (black circles), $\text{Ge}_{10}\text{Se}_{90}$ (black squares), $\text{Ge}_{17}\text{Se}_{83}$ (light gray diamonds), $\text{Ge}_{20}\text{Se}_{80}$ (dark gray triangles), and $\text{Ge}_{23}\text{Se}_{77}$ (light gray squares) supercooled liquids at different T_g -scaled temperatures. τ_{shear} curves from bottom to top are in the order of increasing Ge concentration. τ_{shear} values are obtained from previously published shear viscosity data (Ref. 26) using Maxwell's relation (see text for details).

namics of Se-Se-Se linkages as a consequence of an elastic stiffening of the network. These structural rearrangements involve hopping over barriers in the potential-energy landscape of the supercooled liquid to explore the equilibrium configurations or “inherent” structures. In this dynamical scenario that is consistent with the elastic models of viscous flow, the time scale τ_0 corresponds to that of local elastic deformation of the selenium chain segments that is a precursor to their rotational rearrangement and structural relaxation.^{28,29}

IV. SUMMARY

In summary, the temperature dependence of the ^{77}Se NMR line shapes of $\text{Ge}_x\text{Se}_{100-x}$ supercooled liquids in the glass transition region indicate that the time scale and its temperature dependence for the rotational dynamics of selenium chain segments are practically identical for liquids with $5 \leq x \leq 17$. However, the time scale of this dynamical process slows down abruptly for liquids with $x \geq 20$, across the rigidity percolation threshold. The activation energy of the rotational dynamics remains unchanged but the attempt frequency increases by ~ 1.5 orders of magnitude signifying a transition of the covalent atomic network of the $\text{Ge}_x\text{Se}_{100-x}$ supercooled liquids at the percolation threshold from a floppy to a rigid state.

ACKNOWLEDGMENTS

This work was supported by NSF under Grant No. DMR-0906070 to S.S.

- ¹J. C. Phillips, *J. Non-Cryst. Solids* **34**, 153 (1979).
- ²M. F. Thorpe, *J. Non-Cryst. Solids* **57**, 355 (1983).
- ³H. He and M. F. Thorpe, *Phys. Rev. Lett.* **54**, 2107 (1985).
- ⁴M. Micoulaut and J. C. Phillips, *J. Non-Cryst. Solids* **353**, 1732 (2007).
- ⁵A. K. Varshneya, *J. Non-Cryst. Solids* **273**, 1 (2000).
- ⁶W. A. Kamitakahara, R. L. Cappelletti, P. Boolchand, B. L. Halfpap, F. Gompf, D. A. Neumann, and H. Mutka, *Phys. Rev. B* **44**, 94 (1991).
- ⁷M. Tatsumisago, B. L. Halfpap, J. L. Green, S. M. Lindsay, and C. A. Angell, *Phys. Rev. Lett.* **64**, 1549 (1990).
- ⁸X. Feng, W. J. Bresser, and P. Boolchand, *Phys. Rev. Lett.* **78**, 4422 (1997).
- ⁹M. F. Thorpe, D. J. Jacobs, N. V. Chubynsky, and A. J. Rader, in *Rigidity Theory and Applications*, edited by M. F. Thorpe and P. M. Duxbury (Kluwer, New York, 1999), p. 239.
- ¹⁰S. Stølen, T. Grande, and H. Johnsen, *Phys. Chem. Chem. Phys.* **4**, 3396 (2002).
- ¹¹G. G. Naumis, *J. Non-Cryst. Solids* **352**, 4865 (2006).
- ¹²G. G. Naumis, *Phys. Rev. B* **61**, R9205 (2000).
- ¹³J. C. Mauro, P. K. Gupta, and R. J. Loucks, *J. Chem. Phys.* **130**, 234503 (2009).
- ¹⁴M. M. Smedskjaer, J. C. Mauro, and Y. Yue, *J. Chem. Phys.* **131**, 244514 (2009).
- ¹⁵P. K. Gupta and J. C. Mauro, *J. Chem. Phys.* **130**, 094503 (2009).
- ¹⁶F. J. Bermejo, C. Cabrillo, E. Bychkov, P. Fouquet, G. Ehlers, W. Haussler, D. L. Price, and M. L. Saboungi, *Phys. Rev. Lett.* **100**, 245902 (2008).
- ¹⁷P. Boolchand, X. Feng, and W. J. Bresser, *J. Non-Cryst. Solids* **293-295**, 348 (2001).
- ¹⁸F. Wang, S. Mamedov, P. Boolchand, B. Goodman, and M. Chandrasekhar, *Phys. Rev. B* **71**, 174201 (2005).
- ¹⁹T. Takahashi, H. Kawashima, H. Sugisawa, and T. Baba, *Solid State Nucl. Magn. Reson.* **15**, 119 (1999).
- ²⁰B. Bureau, J. Troles, M. Le Floch, P. Guénot, F. Smektala, and J. Lucas, *J. Non-Cryst. Solids* **319**, 145 (2003).
- ²¹B. Bureau, J. Troles, M. Le Floch, F. Smektala, and J. Lucas, *J. Non-Cryst. Solids* **326-327**, 58 (2003).
- ²²E. L. Gjersing, S. Sen, and B. G. Aitken, *J. Phys. Chem. C* **114**, 8601 (2010).
- ²³C. Rosenhahn, S. Hayes, G. Brunklaus, and H. Eckert, in *Phase Transitions and Self-Organization in Electronic and Molecular Networks*, edited by J. C. Phillips and M. Thorpe (Kluwer Academic/Plenum, New York, 2001), pp. 123–141.
- ²⁴P. Lucas, E. A. King, O. Gulbilen, J. L. Yarger, E. Soignard, and B. Bureau, *Phys. Rev. B* **80**, 214114 (2009).
- ²⁵M. Mehring, *Principles of High Resolution NMR in Solids* (Springer-Verlag, Berlin, 1983).
- ²⁶S. V. Z. Nemilov, *Zh. Prikl. Khim. (S.-Peterburg)* **37**, 1020 (1964).
- ²⁷A. N. Sreeram, A. K. Varshneya, and D. R. Swiler, *J. Non-Cryst. Solids* **128**, 294 (1991).
- ²⁸C. A. Angell, K. L. Ngai, G. B. McKenna, P. F. McMillan, and S. W. Martin, *J. Appl. Phys.* **88**, 3113 (2000).
- ²⁹J. C. Dyre, *Rev. Mod. Phys.* **78**, 953 (2006).